

See discussions, stats, and author profiles for this publication at: <https://www.researchgate.net/publication/5548353>

Pestalothols A–D, Bioactive Metabolites from the Plant Endophytic Fungus *Pestalotiopsis theae*

ARTICLE in JOURNAL OF NATURAL PRODUCTS · MAY 2008

Impact Factor: 3.8 · DOI: 10.1021/np700744t · Source: PubMed

CITATIONS

49

READS

40

6 AUTHORS, INCLUDING:



Tian Renrong

Chinese Academy of Sciences

8 PUBLICATIONS 196 CITATIONS

SEE PROFILE



Xulin Chen

Wuhan Institute Of Virology

59 PUBLICATIONS 955 CITATIONS

SEE PROFILE



Liangdong Guo

Chinese Academy of Sciences

163 PUBLICATIONS 2,873 CITATIONS

SEE PROFILE



Yongsheng Che

Beijing institute of Pharmacology & Toxicology

92 PUBLICATIONS 946 CITATIONS

SEE PROFILE

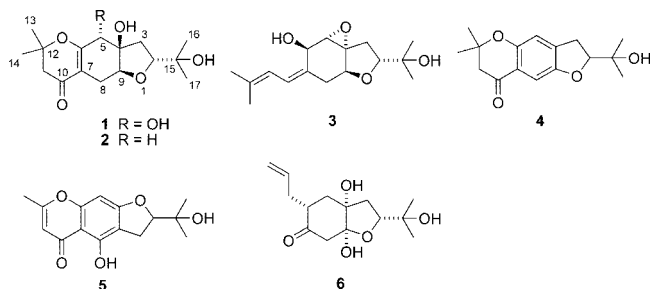
Pestalotheols A–D, Bioactive Metabolites from the Plant Endophytic Fungus *Pestalotiopsis theae*Erwei Li,[†] Renrong Tian,[‡] Shuchun Liu,[†] Xulin Chen,^{*,‡} Liangdong Guo,[†] and Yongsheng Che^{*,†}

Key Laboratory of Systematic Mycology and Lichenology, and Center for Bio-Energy and Industrial Biotechnology, Institute of Microbiology, Chinese Academy of Sciences, Beijing, 100080, People's Republic of China, and State Key Laboratory of Virology, Wuhan Institute of Virology, Chinese Academy of Sciences, Wuhan 430071, People's Republic of China

Received December 24, 2007

Pestalotheols A–D (**1–4**), four new metabolites, have been isolated from cultures of an isolate of the plant endophytic fungus *Pestalotiopsis theae*. The structures of these compounds were determined by NMR spectroscopy, and **1** is further confirmed by X-ray crystallography. The absolute configurations of compounds **1** and **3** were assigned by application of the modified Mosher method. Pestalotheol C (**3**) displayed an inhibitory effect on HIV-1_{LAI} replication in C8166 cells with an EC₅₀ value of 16.1 μ M.

Plant endophytic fungi are well-known as sources of bioactive secondary metabolites.^{1,2} *Pestalotiopsis* species are very common in their distribution, occurring on a wide range of substrata, and many are saprobes, while others are either pathogenic or endophytic on living plant leaves and twigs.³ Chemical investigations of some *Pestalotiopsis* spp. have afforded a variety of bioactive natural products.^{4–14} *Pestalotiopsis theae* is known as a causal fungus for tea gray blight disease, and chemical studies of this fungus have led to the identification of phytotoxins and plant growth regulators.^{15–17} During an ongoing search for new bioactive metabolites from plant endophytic fungi, a subculture of an isolate of *P. theae* (LN560), obtained from branches of an unidentified tree on Jianfeng Mountain, Hainan Province, People's Republic of China, was grown in solid-substrate fermentation culture. Its organic solvent extract displayed an inhibitory effect on HIV-1_{LAI} replication in C8166 cells. Bioassay-guided fractionation of this extract afforded four new compounds, which have been named pestalotheols A–D (**1–4**). Details of the isolation, structure elucidation, and biological activity of these compounds are reported herein.



Results and Discussion

The molecular formula of pestalotheol A (**1**) was determined to be C₁₆H₂₄O₆ (five degrees of unsaturation) by analysis of its HRESIMS (*m/z* 335.1466 [M + Na]⁺; Δ +0.4 mmu) and NMR data (Table 1). Analysis of the ¹H, ¹³C, and HMQC NMR spectroscopic data of **1** revealed the presence of three exchangeable protons, four methyl groups, three methylene units, three oxymethines, three oxygenated quaternary carbons, two olefinic carbons, and one α,β -conjugated carbonyl carbon (δ_C 192.6). These data accounted for all ¹H and ¹³C NMR resonances and required the compound to be tricyclic. Analysis of the ¹H–¹H COSY NMR data

led to the identification of three isolated proton spin-systems corresponding to the C-2–C-3, C-5–C-5–OH, and C-8–C-9 fragments of structure **1**. HMBC correlations from H-2 to C-3 and C-9, from H-3a to C-2 and C-4, and from H-3b to C-4 and C-9 established the tetrahydrofuran subunit. In turn, correlations from H-5 to C-4, C-6, C-7, and C-9, the exchangeable proton at 4.95 ppm to C-4, C-5, and C-6, H₂-8 to C-4, C-6, C-7, and C-9, and H-9 to C-4 and C-5 led to the identification of a reduced furanocyclohexene moiety with a hydroxy group attached to C-5. Other correlations of H₃-16 and H₃-17 with C-2 and C-3 indicated that C-2, C-16, and C-17 are all connected to C-15, while those from H₃-13 and H₃-14 to C-11 and C-12, H₂-11 to C-7 and C-10, and H₂-8 to C-10 completed the C-10–C-14 substructure of **1**, with C-10 directly attached to C-7. Key HMBC correlations from the second exchangeable proton (δ_H 3.86) to C-3, C-4, C-5, and C-9 and the third exchangeable proton (δ_H 3.16) to C-2, C-15, C-16, and C-17 indicated that C-4 and C-15 are attached to free hydroxy groups. Considering the chemical shifts of C-6 (δ_C 167.5) and C-12 (δ_C 80.6), as well as the unsaturation requirement for **1**, C-6 and C-12 have to be connected to the same oxygen atom to form a dihydropyranone moiety. On the basis of these data, the gross structure of pestalotheol A was established as **1**.

The relative configuration of pestalotheol A (**1**) was assigned by analysis of ¹H–¹H coupling constants and NOESY data (Table 1). The large *trans*-diaxial-type coupling constant observed between H-8b and H-9 (11 Hz) indicated that both protons are in pseudoaxial orientations with respect to the corresponding cyclohexene ring. NOESY correlations from the exchangeable proton OH-4 with H-2 and H-8b indicated that these protons are all on the same face of the ring system, whereas correlations from H-9 to OH-5 were used to place them on the opposite face of the molecule, thereby establishing the relative configuration of pestalotheol A as **1**. Ultimately, the structure of **1** was confirmed by X-ray crystallographic analysis, and a perspective ORTEP plot is shown in Figure 1.

The absolute configuration of pestalotheol A (**1**) was assigned by application of the modified Mosher method.^{18,19} Treatment of **1** with (*S*)-MTPA Cl and (*R*)-MTPA Cl afforded the (*R*)-MTPA ester (**1a**) and (*S*)-MTPA ester (**1b**), respectively. The difference in chemical shift values ($\Delta\delta = \delta_S - \delta_R$) for the diastereomeric esters **1b** and **1a** was calculated in order to assign the absolute configuration at C-5. Calculations for all of the relevant signals except one (H₃-16) suggested the *R* absolute configuration at C-5. Therefore, the 2*R*, 4*R*, 5*R*, and 9*S* absolute configuration was proposed for compound **1** on the basis of the $\Delta\delta$ results summarized in Figure 2.

Pestalotheol B (**2**) was assigned a molecular formula of C₁₆H₂₄O₅ (five degrees of unsaturation) on the basis of its HRESIMS (*m/z*

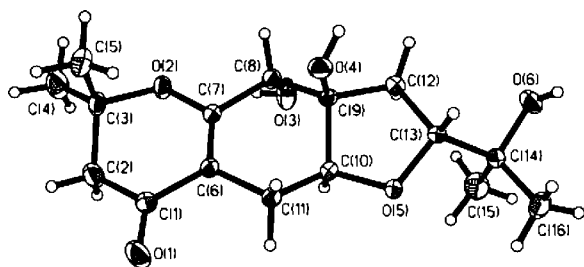
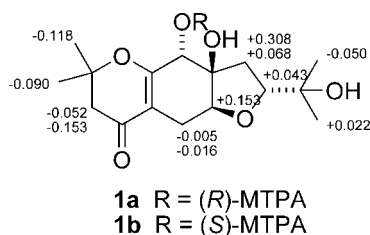
* To whom correspondence should be addressed. Tel: 86 10 82618785. Fax: 86 10 82618785. E-mail: (Y.C.) cheys@im.ac.cn; (X.C.) chenxl@wh.iov.cn.

[†] Institute of Microbiology.

[‡] Wuhan Institute of Virology.

Table 1. NMR Spectroscopic Data of Pestalothol A (**1**) in Acetone- d_6

position	δ_H^a (J in Hz)	δ_C^b , mult.	HMBC (H \rightarrow C#)	NOESY
2	4.12, dd (10, 6.4)	85.8, CH	3, 9, 15, 16, 17	4-OH, 16, 17
3a	2.49, dd (13, 10)	35.2, CH ₂	2, 4, 15	5, 5-OH, 9, 16, 17
3b	1.76, dd (13, 6.4)		4, 9	4-OH, 5
4		80.1, qC		
5	4.08, d (5.7)	72.8, CH	4, 6, 7, 9	3a, 3b
6		167.5, qC		
7		108.6, qC		
8a	2.63, dd (15, 5.7)	22.7, CH ₂	4, 6, 7, 9, 10	
8b	2.12, dd (15, 11)		4, 6, 7, 9, 10	4-OH
9	3.90, dd (11, 5.7)	77.0, CH	4, 5	3a, 5-OH, 16, 17
10		192.6, qC		
11a	2.54, d (16)	47.7, CH ₂	7, 10, 12, 13, 14	
11b	2.37, d (16)		7, 10, 12, 13, 14	
12		80.6, qC		
13	1.41, s	27.8, CH ₃	10, 11, 12, 14	
14	1.33, s	24.5, CH ₃	11, 12, 13	
15		72.1, qC		
16	1.18, s	26.7, CH ₃	2, 15, 17	2, 3a, 9
17	1.09, s	25.6, CH ₃	2, 15, 16	2, 3a, 9
OH-4	3.86, s		3, 4, 5, 9	2, 3b, 8b
OH-5	4.95, d (5.7)		4, 5, 6	3a, 9
OH-15	3.16, s		2, 15, 16, 17	3a

^a Recorded at 400 MHz. ^b Recorded at 100 MHz.**Figure 1.** Thermal ellipsoid representation of **1**.**Figure 2.** $\Delta\delta$ values (in ppm) = $\delta_S - \delta_R$ obtained for (S)- and (R)-MPTA esters **1a** and **1b**.

319.1520 [M + Na]⁺; Δ +0.1 mmu) and NMR data (Tables 2 and 3) Analysis of the ¹H and ¹³C NMR data for **2** revealed the presence of structural features similar to those found in **1**, except that the oxymethine (δ_H/δ_C 4.08/72.8) was replaced by signals for a methylene unit (δ_H/δ_C 2.13, 2.07/41.2) in the NMR spectra of **2**, and this observation was supported by HMBC correlations from these newly observed methylene protons to C-4 and C-7. Therefore, the gross structure of pestalothol B was proposed as **2**. The relative configuration of **2** was assigned by analysis of ¹H–¹H coupling constants, NOESY data, and comparison of its ¹H NMR data with those of pestalothol A (**1**). The absolute configuration of pestalothol B (**2**) was assigned as shown by analogy to pestalothol A (**1**).

The molecular formula of pestalothol C (**3**) was established as C₁₆H₂₄O₄ (five degrees of unsaturation) on the basis of HRESIMS analysis (m/z 303.1569 [M + Na]⁺; Δ +0.3 mmu) and the NMR data (Tables 2 and 3). The ¹H and ¹³C NMR data for **3** differed significantly from those of **1** and **2**, suggesting a substantial structural change. Upon analysis of COSY and HMBC data, the same partial structure of a tetrahydrofuran ring with a 2-hydroxy-

Table 2. ¹H NMR Spectroscopic Data of Pestalothols B–D (**2–4**) in Acetone- d_6

	pestalothol B (2)	pestalothol C (3)	pestalothol D (4)
position	δ_H^a (J in Hz)	δ_H^a (J in Hz)	δ_H (J in Hz)
2	4.10, dd (8.6, 7.5)	4.07, dd (9.4, 6.7)	4.59, dd (8.8, 8.6)
3a	2.53, dd (13, 8.6)	2.54, dd (13, 9.4)	3.28, dd (17, 8.6)
3b	2.00, dd (13, 7.5)	1.71, dd (13, 6.7)	3.18, dd (17, 8.8)
4			
5a	2.13, d (10)	3.74, d (2.7)	6.79, s
5b	2.07, d (10)		
6		4.63 br, d (8.5)	
7			
8a	2.64, dd (15, 5.6)	2.49, t (12)	6.95, s
8b	2.12, dd (15, 11)	2.21, dd (12, 4.8)	
9	3.67, dd (11, 5.6)	3.85, dd (12, 4.8)	
10		6.14, d (11)	
11a	2.49, d (16)	6.24, d (11)	2.66, s
11b	2.37, d (16)		
12			
13	1.39, s	1.78, s	1.40, s
14	1.34, s	1.73, s	1.40, s
15			
16	1.19, s	1.08, s	1.19, s
17	1.06, s	1.23, s	1.25, s
OH-4	3.75, s		
OH-6		3.87, d (8.7)	
OH-15	3.19, s	3.31, s	3.62, s

^a Recorded at 400 MHz.

isopropyl side chain attached at C-2, like that appearing in **1** and **2**, was established. Four isolated proton spin-systems corresponding to the C-2–C-3, C-5–C-6 (including C-6-OH), C-8–C-9, and C-10–C-11 subunits of structure **3** were established by analysis of its COSY NMR data. HMBC correlations from H-5 to C-3 and C-4, H-6 to C-7 and C-8, and H-8b to C-4, C-6, C-7, and C-9 permitted completion of a cyclohexane unit. Key HMBC correlations from H₃-13 and H₃-14 to C-11 and C-12 and from the olefinic proton H-10 to C-6 and C-8 enabled the completion of the C-7–C-14 partial structure of **3**, with C-7 directly attached to C-10. Correlations from the exchangeable proton (δ_H 3.87) to C-5, C-6, and C-7 established the connectivity between C-6 and a hydroxy group. Considering the chemical shifts of C-4 (δ_C 69.5) and C-5 (δ_C 60.1), as well as the unsaturation requirement for **3**, C-4 and C-5 have to be connected to one oxygen atom to form an epoxide moiety. On the basis of these data, the planar structure of pestalothol C was established as depicted in **3**.

Table 3. ^{13}C NMR Spectroscopic Data of Pestalotheols B–D (2–4) in Acetone- d_6

	pestalotheol B (2)	pestalotheol C (3)	pestalotheol D (4)
position	δ_{C}^a , mult.	δ_{C}^a , mult.	δ_{C}^a , mult.
2	85.9, CH	86.0, CH	90.2, CH
3	39.8, CH ₂	31.1, CH ₂	31.6, CH ₂
4	81.3, qC	69.5, qC	139.5, qC
5	41.2, CH ₂	60.1, CH	115.6, CH
6	167.4, qC	64.8, CH	155.7, qC
7	108.4, qC	134.3, qC	119.9, qC
8	22.4, CH ₂	35.4, CH ₂	103.5, CH
9	76.8, CH	77.8, CH	155.3, s qC
10	191.3, qC	128.7, CH	191.9, qC
11	47.7, CH ₂	121.9, CH	49.0, CH ₂
12	80.6, qC	136.2, qC	79.5, qC
13	27.4, CH ₃	26.4, CH ₃	26.7, CH ₃
14	25.2, CH ₃	18.0, CH ₃	26.5, CH ₃
15	72.0, qC	71.9, qC	71.4, qC
16	26.9, CH ₃	25.8, CH ₃	26.0, CH ₃
17	25.6, CH ₃	26.7, CH ₃	25.6, CH ₃

^a Recorded at 100 MHz.

The relative configuration of pestalotheol C (3) was assigned by analysis of ^1H – ^1H coupling constants and NOESY correlations (Figure 3). The large coupling constant observed between H-8a and H-9 (12 Hz) and between H-2 and H-3a (9.4 Hz) suggested a *trans* relationships between adjacent protons. NOESY correlations from H-8a to H-2 and OH-6 and from H-5 to H-3b placed these protons on the same face of the ring system, and correlations of H-9 with H-3a and H-6 indicated that they are on the opposite face of the ring system. NOESY correlations of H-6 with H-11 and of H-8b with H-10 established the *Z*-geometry of the C-7/C-10 double bond. On the basis of these data, the relative configuration of pestalotheol C was established as shown in 3.

The absolute configuration of pestalotheol C (3) was also assigned by application of the modified Mosher method. The differences in chemical shift values ($\Delta\delta = \delta_{\text{S}} - \delta_{\text{R}}$) for the diastereomeric esters **3b** and **3a** were calculated in order to assign the absolute configuration at C-6. Calculations for all of the relevant signals suggested the *R* absolute configuration at C-6, and the 2*R*, 4*R*, 5*S*, 6*R*, and 9*S* absolute configuration was proposed for compound 3 on the basis of the results summarized in Figure 4.

The molecular formula of pestalotheol D (4) was determined to be $\text{C}_{16}\text{H}_{20}\text{O}_4$ (seven unsaturations) by analysis of its HRESIMS (m/z 299.1252 [$\text{M} + \text{Na}]^+$; $\Delta +0.2$ mmu) and NMR data (Tables 2 and 3). Analysis of its NMR data revealed the presence of the same 2-hydroxyisopropyl side chain and dihydropyranone moiety as those present in 1 and 2, except that the signals for four sp^3 carbons, C-4, C-5, C-8, and C-9, were replaced by four aromatic resonances in the NMR spectra of 4, indicating that the cyclohexene ring occurring in 1 and 2 was aromatized. HMBC correlations from H-5 to C-3, C-6, C-7, and C-9 and from H-8 to C-4, C-6, C-9, and C-10 further confirmed the presence of an aromatic ring in 4. The ^{13}C NMR chemical shift of C-9 (δ_{C} 155.3) indicated that it was oxygenated, and an HMBC correlation of H-2 with C-9 established the connectivity of C-2 and C-9 via an oxygen to form a dihydrofuran ring. On the basis of these data, the structure of pestalotheol D was established as depicted in 4.

Pestalotheols A–D (1–4) were tested for in vitro activity against HIV-1_{LAI}. Pestalotheol C (3) showed an inhibitory effect on HIV-1 replication in C8166 cells, with EC_{50} and CC_{50} values of 16.1 and 163 μM , respectively (selectivity index, $\text{SI} = 10.1$; the positive control indinavir sulfate showed an EC_{50} value of 8.18 nM). Pestalotheols A–D (1–4) were also evaluated for activity against a panel of bacteria including *Staphylococcus aureus* (ATCC 6538), *Streptococcus mutans* (ATCC 25175), *Enterococcus faecalis* (ATCC 19433), and *Sarcina lutea* (CMCC B28001), and the fungi *Geotrichum candidum* (AS2.498), *Candida albicans* (ATCC 10231), and *Aspergillus fumigatus* (ATCC 10894). However, none of these

compounds showed noticeable in vitro antimicrobial or antifungal activity when tested at 100 $\mu\text{g}/\text{disk}$.

Pestalotheols A (1), B (2), and D (4) are new members of the chromenone type of metabolites. Biogenetically, these compounds could be derived from two units of isoprenoids and a polyketide, whereas pestalotheol C (3) could be their biosynthetic precursor. Natural products containing a reduced tetrahydro-2*H*-furo[3,2-*g*]chromene unit have been reported previously, such as visaminol (5).²⁰ However, pestalotheols A (1), B (2), and D (4) differ significantly from their naturally occurring precedents in the identity of the substituents and, most notably, in the fused pattern between the cyclohexene (aromatic in 4) moiety and the furan ring. Pestalotheol C (3) is closely related to illifunone E (6)²¹ and illicinone E,²² but differs in the identity of the substituents as well as the presence of an epoxide moiety *cis*-fused to the cyclohexane ring.

Experimental Section

General Experimental Procedures. Optical rotations were measured on a Perkin-Elmer 241 polarimeter, and UV data were recorded on a Hitachi U-2800 spectrophotometer. IR data were recorded using a Bruker Vertex 70 spectrophotometer. ^1H and ^{13}C NMR data were acquired with a Bruker Avance-400 spectrometer using solvent signals (acetone- d_6 ; δ_{H} 2.05/ δ_{C} 29.8, 206.1) as references. The HMQC and HMBC experiments were optimized for 145.0 and 8.0 Hz, respectively. ESIMS data were recorded on a Bruker Esquire 3000Plus spectrometer, and HRESIMS data were obtained using a Bruker APEX III 7.0 T spectrometer.

Fungal Material. The culture of *P. theae* was isolated by one of the authors (L.G.) from the branches of an unidentified tree near the Jianfeng Mountain, Hainan Province, in April 2005. The isolate was identified and assigned the accession number LN560 in L.G.'s culture collection at the Institute of Microbiology, Chinese Academy of Sciences, Beijing. The fungal strain was cultured on slants of potato dextrose agar (PDA) at 25 °C for 10 days. Fermentation was carried out in four 500 mL Fernbach flasks each containing 100 g of rice. Spore inoculum was prepared by suspension in sterile, distilled H₂O to give a final spore/cell suspension of $1 \times 10^6/\text{mL}$. Distilled H₂O (100 mL) was added to each flask, and the contents were soaked overnight before autoclaving at 15 lb/in.² for 30 min.²³ After cooling to room temperature, each flask was inoculated with 5.0 mL of the spore inoculum and incubated at 25 °C for 40 days.

Extraction and Isolation. The fermented rice substrate was extracted repeatedly with MEK (3 \times 500 mL), and the organic solvent was evaporated to dryness under vacuum to afford 2.51 g of crude extract. The extract was fractionated by silica gel VLC using petroleum ether–EtOAc gradient elution. The fraction (26 mg) eluted with 15% EtOAc was further separated by semipreparative reversed-phase HPLC (Kramosil C₁₈ column; 10 μm ; 10 \times 250 mm; 2 mL/min) to afford pestalotheol D (4; 4.5 mg, t_{R} 18.4 min; 60 to 80% CH₃OH in water over 30 min). The fractions eluted with 30% (50 mg), 50% (100 mg), 55% (140 mg), and 60% (150 mg) EtOAc were fractionated again by Sephadex LH-20 column chromatography using CHCl₃–CH₃OH (1:1) as eluents. Purification of these fractions with different gradients afforded pestalotheols A (1; 30.0 mg, t_{R} 11.8 min; 30 to 60% CH₃OH in water over 35 min), B (2; 4.5 mg, t_{R} 16.0 min; 40 to 55% CH₃OH in water over 25 min), and C (3; 9.0 mg, t_{R} 17.2 min; 55 to 75% CH₃OH in water over 30 min).

Pestalotheol A (1): colorless needles, mp 223–225 °C; [α]_D +122 (*c* 1.17, CH₃OH); UV (CH₃OH) λ_{max} 278 (ϵ 6500) nm; IR (neat) ν_{max} 3391 (br), 2976, 1650, 1595, 1373, 1258, 1165, 1085, 1052 cm^{-1} ; ^1H , ^{13}C NMR, HMBC, and NOESY data, see Table 1; HRESIMS obsd m/z 335.1466 [$\text{M} + \text{Na}]^+$ (calcd for $\text{C}_{16}\text{H}_{24}\text{O}_6\text{Na}$, 335.1470).

X-ray Crystallographic Analysis of Pestalotheol A (1).²⁴ Upon crystallization from MeOH–H₂O (10:1) using the vapor diffusion method, colorless crystals were obtained for 1, a crystal (0.26 \times 0.24 \times 0.18 mm) was separated from the sample and mounted on a glass fiber, and data were collected using a Bruker SMART 1000 CCD diffractometer with graphite-monochromated Mo K α radiation, $\lambda = 0.71073$ Å at 294(2) K. Crystal data: $\text{C}_{16}\text{H}_{24}\text{O}_6$, $M = 312.35$, space group orthorhombic, $P2_12_12_1$; unit cell dimensions $a = 6.465(2)$ Å, $b = 10.184(4)$ Å, $c = 25.525(9)$ Å, $V = 1680.6(10)$ Å³, $Z = 4$, $D_{\text{calcd}} = 1.234$ mg/m³, $\mu = 0.094$ mm^{−1}, $F(000) = 672$. The structure was solved

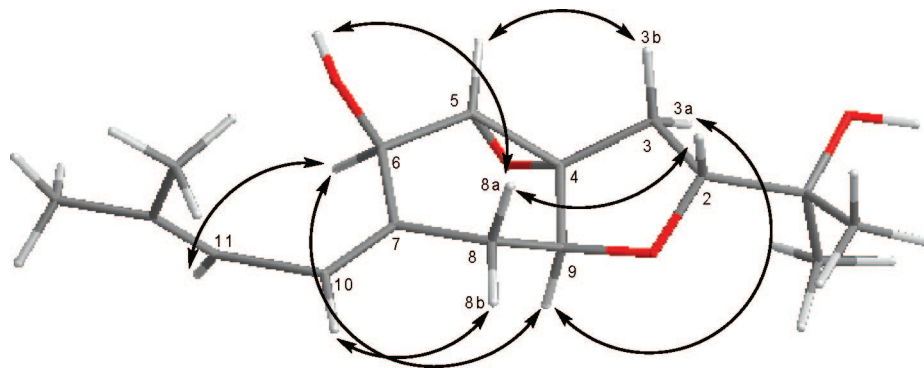


Figure 3. Key NOESY correlations for pestalothel C (3).

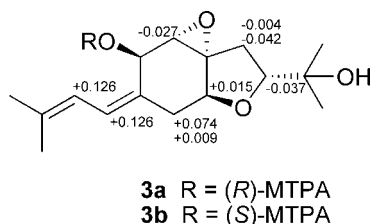


Figure 4. $\Delta\delta$ values (in ppm) = $\delta_S - \delta_R$ obtained for (S)- and (R)-MPTA esters **3a** and **3b**.

by direct methods using SHELXL-97²⁵ and refined using full-matrix least-squares difference Fourier techniques. All non-hydrogen atoms were refined with anisotropic displacement parameters, and all hydrogen atoms were placed in idealized positions and refined as riding atoms with the relative isotropic parameters. Absorption corrections were applied with the Siemens Area Detector Absorption Program (SADABS).²⁶ The 9269 measurements yielded 3477 independent reflections after equivalent data were averaged, and Lorentz and polarization corrections were applied. The final refinement gave $R_1 = 0.0524$ and $wR_2 = 0.1156$ [$I > 2\sigma(I)$].

Preparation of (R)-MTPA Ester (1a) and (S)-MTPA Ester (1b).

A solution of **1** (2.0 mg, 0.006 mmol) in CH_3OH was transferred to a clean NMR tube, and then the solvent was completely removed under vacuum. Pyridine- d_5 (0.5 mL) and (S)-MTPA Cl (9.5 μL , 0.050 mmol) were quickly added, and all contents were mixed thoroughly by shaking the NMR tube carefully. The reaction was performed at room temperature and monitored by ^1H NMR at each 24 h. The reaction was found to be complete at 48 h. The mixture was evaporated to dryness and purified by semipreparative reversed-phase HPLC (Kra-mosil C_{18} column; 10 μm ; 10 \times 250 mm; 2 mL/min, 30 to 100% CH_3OH in H_2O over 35 min, then 100% CH_3OH over 5 min) to afford **1a** (1.9 mg, t_R 37.4 min): white powder; ^1H NMR (acetone- d_6 , 400 MHz) δ 5.65 (1H, s, H-5), 4.55 (1H, s, OH-12), 4.11 (1H, dd, $J = 9.2$, 6.8 Hz, H-2), 3.73 (1H, dd, $J = 11$, 5.5 Hz, H-9), 3.13 (1H, s, OH-15), 2.69 (1H, dd, $J = 16$, 5.6 Hz, H-8a), 2.66 (1H, d, $J = 16$ Hz, H-11a), 2.48 (1H, d, $J = 16$ Hz, H-11b), 2.18 (1H, dd, $J = 16$, 11 Hz, H-8b), 1.91 (1H, dd, $J = 12$, 9.2 Hz, H-3a), 1.88 (1H, dd, $J = 12$, 6.8 Hz, H-3b), 1.48 (3H, s, H-13), 1.32 (3H, s, H-14), 1.09 (3H, s, H-16), 0.94 (3H, s, H-17); ESIMS m/z [$\text{M} + \text{Na}$] $^+$ 551.2.

In a similar fashion, a sample of compound **1** (2.0 mg, 0.006 mmol), pyridine- d_5 (0.5 mL), and (R)-MPTA Cl (9.5 μL , 0.050 mmol) were allowed to react in an NMR tube at ambient temperature for 48 h, and the reaction mixture was processed as described above for **1a** to afford **1b** (1.5 mg): gum; ^1H NMR (acetone- d_6 , 400 MHz) δ 5.62 (1H, s, H-5), 4.54 (1H, s, OH-12), 4.15 (1H, dd, $J = 9.5$, 6.4 Hz, H-2), 3.88 (1H, dd, $J = 11$, 5.5 Hz, H-9), 3.34 (1H, s, OH-15), 2.69 (1H, dd, $J = 16$, 5.6 Hz, H-8a), 2.60 (1H, d, $J = 16$ Hz, H-11a), 2.32 (1H, d, $J = 16$ Hz, H-11b), 2.23 (1H, dd, $J = 12$, 9.6 Hz, H-3a), 2.16 (1H, dd, $J = 16$, 11 Hz, H-8b), 1.94 (1H, dd, $J = 12$, 6.4 Hz, H-3b), 1.37 (3H, s, H-13), 1.23 (3H, s, H-14), 1.04 (3H, s, H-16), 0.97 (3H, s, H-17); ESIMS m/z [$\text{M} + \text{Na}$] $^+$ 551.1.

Pestalothel B (2): colorless needles, mp 214–216 $^\circ\text{C}$; [α] $_D +86$ (c 0.30, CH_3OH); UV (CH_3OH) λ_{max} 276 (ϵ 8000) nm; IR (neat) ν_{max} 3435 (br), 2975, 1650, 1591, 1412, 1372, 1259, 1166, 1085 cm^{-1} ; ^1H and ^{13}C NMR data, see Tables 2 and 3; HMBC data (acetone- d_6 , 400

MHz) H-2 \rightarrow C-3, 4, 16, 17; H-3a \rightarrow C-4, 9; H-3b \rightarrow C-2, 4, 9, 15; H₂-5 \rightarrow C-4, 7; H-8a \rightarrow C-4, 6, 7, 9, 10; H-8b \rightarrow C-4, 7; H₂-11 \rightarrow C-7, 10, 12, 13, 14; H₃-13 \rightarrow C-11, 12, 14; H₃-14 \rightarrow C-11, 12, 13; H₃-16 \rightarrow C-2, 15, 17; H₃-17 \rightarrow C-2, 15, 16; OH-4 \rightarrow C-3, 4, 5, 9; OH-15 \rightarrow C-2, 15, 16, 17; key NOESY correlations (acetone- d_6 , 400 MHz) H-2 \leftrightarrow OH-4, H₃-16, H₃-17; H-3a \leftrightarrow H-5a, H-9; H-5a \leftrightarrow H-3a, 9; H-9 \leftrightarrow H-3a, H-5a, H₃-16, H₃-17; OH-4 \leftrightarrow H-2, H-3b, H-5b; HRESIMS obsd m/z 319.1520 [$\text{M} + \text{Na}$] $^+$ (calcd for $\text{C}_{16}\text{H}_{24}\text{O}_5\text{Na}$, 319.1521).

Pestalothel C (3): colorless powder; [α] $_D +230$ (c 0.60, CH_3OH); UV (CH_3OH) λ_{max} 247 (ϵ 16 600) nm; IR (neat) ν_{max} 3435 (br), 2972, 2922, 1376, 1053, 1018 cm^{-1} ; ^1H and ^{13}C NMR data, see Tables 2 and 3; HMBC data (acetone- d_6 , 400 MHz) H-2 \rightarrow C-3, 9, 15, 16, 17; H-3a \rightarrow C-2, 4, 5, 15; H-3b \rightarrow C-4, 9; H-5 \rightarrow C-3, 4, 6, 7, 10; H-6 \rightarrow C-7, 8, 10; H-8b \rightarrow C-4, 6, 7, 9, 10; H-9 \rightarrow C-4; H-10 \rightarrow C-6, 8; H₃-13 \rightarrow C-10, 11, 12, 14; H₃-14 \rightarrow C-10, 11, 12, 13; H₃-16 \rightarrow C-2, 15, 17; H₃-17 \rightarrow C-2, 15, 16; OH-6 \rightarrow C-5, 6, 7; OH-15 \rightarrow C-2, 15, 16, 17; key NOESY correlations (acetone- d_6 , 400 MHz) H-2 \leftrightarrow H-8a, H₃-16, H₃-17; H-3a \leftrightarrow H-9; H-3b \leftrightarrow H-5; H-5 \leftrightarrow H-3b; H-6 \leftrightarrow H-9, H-11; H-8a \leftrightarrow H-2, OH-6; H-8b \leftrightarrow H-10; H-9 \leftrightarrow H-3a, H-6, H₃-16; HRESIMS obsd m/z 303.1569 [$\text{M} + \text{Na}$] $^+$ (calcd for $\text{C}_{16}\text{H}_{24}\text{O}_4\text{Na}$, 303.1572).

Preparation of (R)-MTPA Ester (3a) and (S)-MTPA Ester (3b).

A sample of **3** (1.0 mg, 0.003 mmol), (S)-MPTA Cl (5.0 μL , 0.026 mmol), and pyridine- d_5 (0.5 mL) were allowed to react in an NMR tube at ambient temperature for 24 h, with the ^1H NMR data of the R-MPTA ester derivative (**3a**) were obtained directly on the reaction mixture: ^1H NMR (pyridine- d_5 , 400 MHz) δ 6.10 (1H, br s, H-6), 6.00 (1H, d, $J = 12$ Hz, H-11), 5.80 (1H, d, $J = 12$ Hz, H-10), 4.19 (1H, dd, $J = 9.2$, 6.8 Hz, H-2), 4.08 (1H, d, $J = 2.8$ Hz, H-5), 3.93 (1H, dd, $J = 12$, 4.8 Hz, H-9), 2.67 (1H, dd, $J = 12$, 9.2 Hz, H-3a), 2.64 (1H, t, $J = 12$ Hz, H-8a), 2.17 (1H, dd, $J = 12$, 4.8 Hz, H-8b), 1.76 (1H, dd, $J = 12$, 6.8 Hz, H-3b), 1.53 (3H, s, H-13), 1.39 (3H, s, H-14), 1.30 (3H, s, H-16), 1.07 (3H, s, H-17).

Similarly, the reaction mixture from another sample of **3** (1.0 mg, 0.003 mmol), (R)-MPTA Cl (5.0 μL , 0.026 mmol), and pyridine- d_5 (0.5 mL) was processed as described above for **3a** to afford **3b**: ^1H NMR (pyridine- d_5 , 400 MHz) δ 6.18 (1H, br s, H-6), 6.13 (1H, d, $J = 12$ Hz, H-11), 5.93 (1H, d, $J = 12$ Hz, H-10), 4.15 (1H, dd, $J = 8.4$, 7.2 Hz, H-2), 4.05 (1H, d, $J = 2.0$ Hz, H-5), 3.95 (1H, dd, $J = 12$, 4.8 Hz, H-9), 2.68 (1H, dd, $J = 14$, 9.2 Hz, H-3a), 2.64 (1H, t, $J = 14$ Hz, H-8a), 2.24 (1H, dd, $J = 14$, 4.8 Hz, H-8b), 1.71 (1H, dd, $J = 14$, 6.4 Hz, H-3b), 1.51 (3H, s, H-13), 1.46 (3H, s, H-14), 1.29 (3H, s, H-16), 1.06 (3H, s, H-17).

Pestalothel D (4): gum; [α] $_D -11$ (c 0.20, CH_3OH); UV (CH_3OH) λ_{max} 237 (ϵ 7800), 264 (ϵ 2800), 366 (ϵ 2000) nm; IR (neat) ν_{max} 3436, 2974, 1680, 1628, 1448, 1371, 1256, 1165, 897 cm^{-1} ; ^1H and ^{13}C NMR data, see Tables 2 and 3; HMBC data (acetone- d_6 , 400 MHz) H-2 \rightarrow C-4, 9, 16, 17; H₂-3 \rightarrow C-2, 4, 5, 9, 15; H-5 \rightarrow C-3, 6, 7, 9; H-8 \rightarrow C-4, 6, 9, 10; H₂-11 \rightarrow C-7, 10, 12, 13, 14; H₃-13 \rightarrow C-10, 11, 12, 14; H₃-14 \rightarrow C-10, 11, 12, 13; H₃-16 \rightarrow C-2, 15, 17; H₃-17 \rightarrow C-2, 15, 16; OH-15 \rightarrow C-2, 15, 16, 17; HRESIMS obsd m/z 299.1252 [$\text{M} + \text{Na}$] $^+$ (calcd for $\text{C}_{16}\text{H}_{20}\text{O}_4\text{Na}$, 299.1259).

Antimicrobial and Antifungal Bioassays. Antimicrobial and antifungal bioassays were conducted according to a literature procedure.²⁷ The bacterial strains were grown on Mueller-Hinton agar, the yeasts *Candida albicans* (ATCC 10231) and *Geotrichum candidum* (AS2.498)

were grown on Sabouraud dextrose agar, and the fungus, *Aspergillus fumigatus* (ATCC 10894), was grown on potato dextrose agar. Test compounds were absorbed onto individual paper disks (6 mm diameter) at 100 µg/disk and placed on the surface of agar. The assay plates were incubated at 25 °C for 48 h (at 37 °C for 24 h for antimicrobial activity) and examined for the presence of a zone of inhibition.

Anti-HIV Assays. Anti-HIV assays included cytotoxicity and HIV-1 replication inhibition evaluations. The cytotoxicity was measured by the MTT method as described in the literature.²⁸ Cells (3×10^4 /well) were seeded into a 96-well microtiter plate in the absence or presence of various concentrations of test compounds in triplicate and incubated at 37 °C in a humid atmosphere of 5% CO₂. After a 4-day incubation, cell viability was measured by the 3-(4,5-dimethylthiazol-2-yl)-2,5-diphenyltetrazolium bromide (MTT) method. The concentration that caused the reduction of viable cells by 50% (CC₅₀) was determined. In parallel with the MTT assay, a HIV-1 replication inhibition assay was determined by p24 antigen capture ELISA.²⁹ C8166 cells were exposed to HIV-1_{LAI} (MOI = 0.058) at 37 °C for 1.5 h, washed with PBS to remove free viruses, and then seeded into a 96-well microtiter plate at 3×10^4 cells per well in the absence or presence of test compounds (indinavir sulfate was used as positive control). After 4 days, the supernatant was collected and inactivated by 0.5% Triton X-100. The supernatant was diluted three times, added to the plate coating with anti-p24 McAb (provided by Dr. Bin Yan, Wuhan Institute of Virology, Wuhan, People's Republic of China), and incubated at 37 °C for 1 h. After washing 5 times with PBST, and the HRP-labeled anti-p24 antibody (provided by Dr. Bin Yan) was added and incubated at 37 °C for 1 h. The plate was washed 5 times with PBST, followed by adding OPD reaction mixture. The assay plate was read at 490 nm using a microplate reader within 30 min. The inhibition rate and the EC₅₀ based on p24 antigen expression level were calculated, and the selective index was calculated as CC₅₀/EC₅₀.

Acknowledgment. We gratefully acknowledge financial support from the Key Program of National Hi-Tech Research and Development (Grant 2007AA021506), the Key Project of Chinese Academy of Sciences (Grant KSCX2-Y-G-013), and the National Natural Science Foundation of China (Grant 30670055).

Supporting Information Available: ¹H and ¹³C NMR spectra of pestalothols A–D (1–4). This material is available free of charge via the Internet at <http://pubs.acs.org>.

References and Notes

- Schulz, B.; Boyle, C.; Draeger, S.; Rommert, A.-K.; Krohn, K. *Mycol. Res.* **2002**, *106*, 996–1004.
- Strobel, G. A. *Microbes Infect.* **2003**, *5*, 535–544.
- Jeewon, R.; Liew, E. C. Y.; Simpson, J. A.; Hodgkiss, I. J.; Hyde, K. D. *Mol. Phylogenet. Evol.* **2003**, *27*, 372–383.
- Venkatasubbiah, P.; Van Dyke, C. G. *Phytochemistry* **1991**, *30*, 1471–1474.
- Pulici, M.; Sugawara, F.; Koshino, H.; Uzawa, J.; Yoshida, S.; Lobkovsky, E.; Clardy, J. *J. Org. Chem.* **1996**, *61*, 2122–2124.
- Lee, J. C.; Strobel, G. A.; Lobkovsky, E.; Clardy, J. *J. Org. Chem.* **1996**, *61*, 3232–3233.
- Pulici, M.; Sugawara, F.; Koshino, H.; Uzawa, J.; Yoshida, S. *J. Nat. Prod.* **1996**, *59*, 47–48.
- Pulici, M.; Sugawara, F.; Koshino, H.; Okada, G.; Esumi, Y.; Uzawa, J. *Phytochemistry* **1997**, *46*, 313–319.
- Ogawa, T.; Ando, K.; Aotani, Y.; Shinoda, K.; Tanaka, T.; Tsukuda, E.; Yoshida, M.; Matsuda, Y. *J. Antibiot.* **1995**, *48*, 1401–1406.
- Li, T. Y.; Harper, J. K.; Grant, D. M.; Tombe, B. O.; Bharat, B.; Hess, W. M.; Strobel, G. A. *Phytochemistry* **2001**, *56*, 463–468.
- Li, T. Y.; Strobel, G. A. *Phytochemistry* **2001**, *57*, 261–265.
- Strobel, G.; Ford, E.; Worapong, J.; Harper, J. K.; Arif, A. M.; Grant, D. M.; Fung, P. C. W.; Wh Chau, R. M. W. *Phytochemistry* **2002**, *60*, 179–183.
- Magnani, R. F.; Rodrigues-Fo, E.; Daolio, C.; Ferreira, A. G.; de Souza, A. Q. L. *Z. Naturforsch.* **2003**, *58C*, 319–324.
- Deyrup, S. T.; Swenson, D. C.; Gloer, J. B.; Wicklow, D. T. *J. Nat. Prod.* **2006**, *69*, 608–611.
- Nagata, N.; Ando, Y.; Hirota, A. *Biosci. Biotech. Biochem.* **1992**, *56*, 810–811.
- Kimura, Y.; Kouge, A.; Nakamura, K.; Koshino, H.; Uzawa, J.; Fujioka, S.; Kawano, T. *Biosci. Biotech. Biochem.* **1998**, *62*, 1624–1626.
- Shimada, A.; Takahashi, I.; Kawano, T.; Kimura, Y. *Z. Naturforsch.* **2001**, *56B*, 797–803.
- Dale, J. A.; Mosher, H. S. *J. Am. Chem. Soc.* **1973**, *95*, 512–519.
- Ohtani, I.; Kusumi, T.; Kashman, Y.; Kakisawa, H. *J. Am. Chem. Soc.* **1991**, *113*, 4092–4096.
- Sasaki, H.; Taguchi, H.; Endo, T.; Yosioka, I. *Chem. Pharm. Bull.* **1982**, *30*, 3555–3562.
- Fukuyama, Y.; Shida, N.; Hata, Y.; Kodama, M. *Phytochemistry* **1994**, *36*, 1497–1503.
- Kouno, I.; Shimamoto, S.; Jiang, Z. H.; Tanaka, T. *Phytochemistry* **1997**, *46*, 389–392.
- Che, Y.; Gloer, J. B.; Wicklow, D. T. *J. Nat. Prod.* **2002**, *65*, 399–402.
- Crystallographic data for compound **1** have been deposited with the Cambridge Crystallographic Data Centre (deposition number CCDC 665253). Copies of the data can be obtained, free of charge, on application to the director, CCDC 12 Union Road, Cambridge CB2 1EZ, UK (fax: +44 1223 336033 ore-mail: deposit@ccdc.cam.ac.uk).
- Sheldrick, G. M. *SHELXL-97, Program for X-ray Crystal Structure Solution and Refinement*; University of Göttingen: Göttingen: Germany, 1997.
- Sheldrick, G. M. *SADABS, Program for Empirical Absorption Correction of Area Detector Data*; University of Göttingen: Göttingen, Germany, 1999.
- Wicklow, D. T.; Joshi, B. K.; Gamble, W. R.; Gloer, J. B.; Dowd, P. F. *Appl. Environ. Microbiol.* **1998**, *64*, 4482–4484.
- Zheng, Y. T.; Zhang, W. F.; Ben, K. L.; Wang, J. H. *Immunopharm. Immunot.* **1995**, *17*, 69–79.
- Zhang, G. H.; Wang, Q.; Chen, J. J.; Zhang, X. M.; Tam, S. C.; Zheng, Y. T. *Biochem. Biophys. Res. Commun.* **2005**, *334*, 812–816.

NP700744T